

(Preprint) AAS 13-078

THE MARS SCIENCE LABORATORY (MSL) ENTRY, DESCENT AND LANDING INSTRUMENTATION (MEDLI): HARDWARE PERFORMANCE AND DATA RECONSTRUCTION

Alan Little^{*}, Deepak Bose[†], Chris Karlgaard[‡], Michelle Munk^{*}, Chris Kuhl^{*}, Mark Schoenenberger^{*}, Chuck Antill^{*}, Ron Verhappen[§], and Prasad Kutty[‡], and Todd White^{}**

The Mars Science Laboratory (MSL) Entry, Descent and Landing Instrumentation (MEDLI) hardware was a first-of-its-kind sensor system that gathered temperature and pressure readings on the MSL heatshield during Mars entry on August 6, 2012. MEDLI began as a challenging instrumentation problem, and has been a model of collaboration across multiple NASA organizations. After the culmination of almost 6 years of effort, the sensors performed extremely well, collecting data from before atmospheric interface through parachute deploy. This paper will summarize the history of the MEDLI project and hardware development, including key lessons learned that can apply to future instrumentation efforts. MEDLI returned an unprecedented amount of high-quality engineering data from a Mars entry vehicle. We will present the performance of the 3 sensor types: pressure, temperature, and isotherm tracking, as well as the performance of the custom-built sensor support electronics. A key component throughout the MEDLI project has been the ground testing and analysis effort required to understand the returned flight data. Although data analysis is ongoing through 2013, this paper will reveal some of the early findings on the aerothermodynamic environment that MSL encountered at Mars, the response of the heatshield material to that heating environment, and the aerodynamic performance of the entry vehicle. The MEDLI data results promise to challenge our engineering assumptions and revolutionize the way we account for margins in entry vehicle design.

INTRODUCTION

The Mars Science Laboratory (MSL) Entry Descent and Landing Instrumentation (MEDLI) Project is a heatshield instrumentation suite that was added to the flagship Mars Science Laboratory (MSL) Mission in November 2006. MEDLI as a project with participation by three Mission Directorates as well as contributions from three NASA centers had some unique challenges. The

^{*} NASA Langley Research Center, Mail Stop 489, Hampton VA 23681

[†] NASA Ames Research Center, Moffett Field, CA 94035

[‡] Analytical Mechanics Associates, Mail Stop 489, Hampton VA 23681

[§] Science Systems and Applications Inc., 1 Enterprise Parkway, Suite 200, Hampton VA 23666

^{**} ERC Inc., Moffett Field, CA 94035

Science Mission Directorate provided the vehicle and assumed the technical risk to the MSL mission, Exploration Systems Mission Directorate and later the Office of the Chief Technologist provided the funding for the MEDLI flight system, and the Aeronautics Research Mission Directorate and later the Office of the Chief Technologist provided funding for data processing and analysis. MEDLI provides the first non-Earth entry aeroheating data since the Pathfinder mission, and provides more than an order of magnitude more data than all previous Mars entry missions combined. The acquired data will help answer some of the fundamental questions relating to leeside turbulent heating levels, forebody transition, and thermal protection system material response in a carbon dioxide atmosphere, and permit a more accurate MSL trajectory reconstruction, as well as enable separation of aerodynamic and atmospheric uncertainties in the hypersonic and supersonic regimes.

MEDLI instrumentation consists of three main subsystems: 1) MEDLI Integrated Sensor Plugs (MISP) that is a series of seven 33 mm (1.3 in.) diameter heatshield thermal protection system plugs with embedded thermocouples and recession sensors, 2) Mars Entry Atmospheric Data System (MEADS) that is a series of seven 2.54 mm (0.1 in.) through-holes, or ports, in the thermal protection system that connect via stainless steel tubing to pressure transducers, and 3) the Sensor Support Electronics (SSE) box that conditions sensor signals and provides power to MISP and MEADS. After signal conditioning, the digital signals from the MEDLI instrumentation were transmitted to the Descent Stage Power and Analog Module (DPAM) system located in the descent stage of MSL and the data was stored onboard the rover Curiosity.¹

The MEDLI Sensor System Electronics (SSE) and Mars Atmospheric Entry Data System (MEADS) were built in-house at Langley Research Center and the MEDLI Integrated Sensor Plugs (MISP), the third subsystem, was built in-house at Ames Research Center.

Looking at the heatshield layout, the MEDLI sensors are strategically placed in specific areas determined to provide the best overall picture of the aerothermal state of the heatshield during the entry phase of the mission. As shown in Figure 1, the MEDLI sensors are arranged such that they provide data on areas of interest according to predicted entry conditions. In this figure, colors designate relative temperatures (with the greens being the coolest and reds being the warmest) and the lines designate flow over the heatshield surface (streamlines).

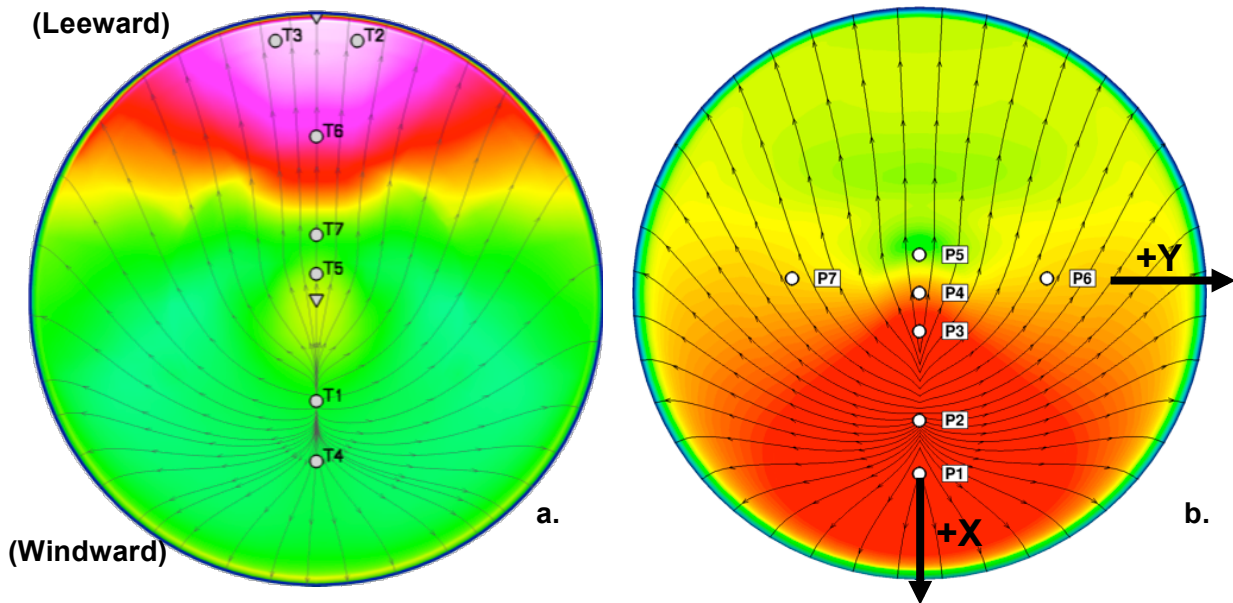


Figure 1 MEDLI sensor layout (viewing outer heatshield surface) illustrating predicted temperatures and pressures (a) MISP layout (b) MEADS layout

Sensors P1, P2, T1, and T4 are located near the expected stagnation point of the flow (T1 is ideally at the stagnation point), so these sensors measure information in this critical flow region; sensors T2, T3, and T6 are located leeward of the turbulent transition region, so these sensors measure the areas of largest aerothermal heating; and sensors P3, P4, P5, P6, P7, T5, and T7 are located in regions of mid-range temperatures and pressures, so these measurements enable the determination of thermal and pressure gradients between the laminar and turbulent flow regimes. Also, the symmetry of the P6 and P7 locations about the central vehicle axis enables the determination of the vehicle angle of sideslip (roll about the +X axis) by interpreting the differential pressure readings from the sensors.

MEDLI's start 6 months prior to the MSL Aeroshell Critical Design Review required the team to work quickly and implement an efficient development process. The Project implemented an approach to design to the MSL interfaces that provided time to complete the interface design, which was an MSL priority, and demonstrate that the risk to MSL was acceptable.

The MEDLI team encountered and overcame numerous obstacles during the development process:

- MSL made the decision to switch Thermal Protection System (TPS) materials from Super Lightweight Ablator (SLA) to Phenolic Impregnated Carbon Ablator (PICA) and redesign the MSL heatshield in October 2007. This change had a significant effect on the MEDLI project, forcing a complete project replan, dictated even closer coordination with MSL as the heatshield TPS design evolved, required an additional design, analysis, and qualification cycle, and the development and delivery of a second set of MEDLI flight hardware to support a parallel MSL system test path.
- A systemic mechanical design flaw was uncovered during SSE vibration testing and MEDLI was able to correct the design flaw through an extensive design by test program.
- Failure of a MEADS transducer prior to final calibration that required a late adjustment to the flight transducer array.
- MSL made a request to the MEDLI project in late October 2008 to evaluate MEDLI's ability to deliver the MISP subsystem approximately 2 months early to take advantage of a schedule opportunity in the heatshield fabrication flow. The MISP hardware was completed and delivered 2 months early in November 2008.

MEDLI INSTRUMENTED SENSOR PLUG (MISP) DEVELOPMENT

MISP consists of seven instrumented plugs integrated into the MSL heatshield. The integrated sensor plugs include layers of thermocouples and a recession sensor. The stacked thermocouples record heating data at varying levels in the heatshield. The recession sensors measure the thickness of the thermal protection system as it ablates during atmospheric entry.

The MISP instrumentation is embedded in 33 mm (1.3 in.) diameter and 29 mm (1.14 in.) deep PICA cylindrical plugs. Each MISP plug contained four Type-K (chromel-alumel) thermocouples with 0.3 mm (0.012 in.) wire diameter at nominal depths of 2.54, 5.08, 11.43, and 17.78 mm (0.1, 0.2, 0.45, and 0.7 in.) from the outer surface as shown in Figure 2a and b. The near surface thermocouple depths are chosen to provide adequate response to any changes in surface heating without burning-off too early in the heat pulse. The deeper thermocouples are embedded in the virgins and pyrolysis zones (illustrated in Figure 3a). In addition to the thermocouples, an ablation sensor, named the HEAT sensor (Hollow aErothermal Ablation and Temperature)² is also

installed through the thickness as shown in Figure 2. This sensor is an improvised version of the ARAD sensor employed for recession measurements in Galileo's entry probe to Jupiter. The HEAT sensor consists of two platinum-tungsten (Pt-W) wires wound around a PICA filled Kapton, a polyimide insulator, tube. As the sensor is heated, the Kapton tube chars and becomes electrically conductive. This conductive path shorts the wires at the char front whose location can be detected by a resistance measurement. The HEAT sensor is shown to follow the time progression of an isotherm through the thickness of the TPS as the material is heated during atmospheric entry. The isotherm temperature that the HEAT sensor follows corresponds to the temperature at which the Kapton has sufficiently charred to establish a conductive path between the two Pt-W wires.

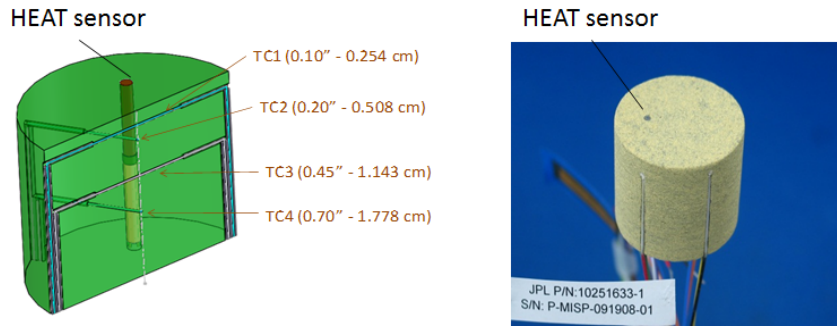


Figure 2 (a) Schematic of a MISP plug with four Type-K thermocouples and a HEAT sensor (b) MISP plug made with PICA

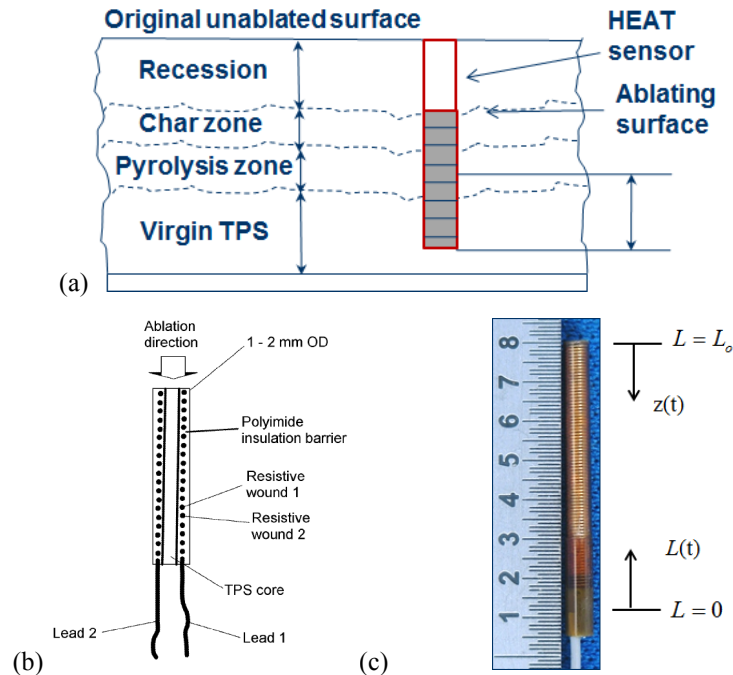


Figure 3 (a) Schematic of a HEAT sensor installed in an ablator, (b) schematic of a HEAT sensor, and (c) HEAT sensor fabricated for MISP plugs

The layout of the MISP plugs on the heatshield is shown in Figure 1a. Each plug is installed using the RTV-560 silicone-elastomer bonding agent as shown in Figure 4a. Figure 4b shows the installation of MEDLI interfaces on the inner side of the heatshield and Figure 4c shows the tiled MSL heatshield with MISP plugs installed. MISP 1 & 4 (T1 & T4) are installed in the stagnation region of the forebody while MISP 5 & 7 (T5 & T7) are embedded in the apex region to capture maximum laminar heating. MISP 2, 3, & 6 (T2, T3, & T6) are located in the leeward forebody to capture turbulent heating levels, as this region is expected to experience maximum heat flux. The plugs are arranged along or near the line of symmetry to capture the development and progression of turbulent flow. MISP 2 & 3 (T2 & T3) are installed slightly away from the centerline to assess asymmetric heating due to any sideslip angle. The strategic placement of the plugs is driven the requirement to address the key aerothermal and TPS uncertainty margins. Substantial margins on stagnation point heating, turbulent heating augmentation and TPS recession are applied during heatshield design. The sensor layout is also expected to address inherent conservatism in the baseline model such as the assumption of a fully turbulent flow and a supercatalytic gas-surface interaction.

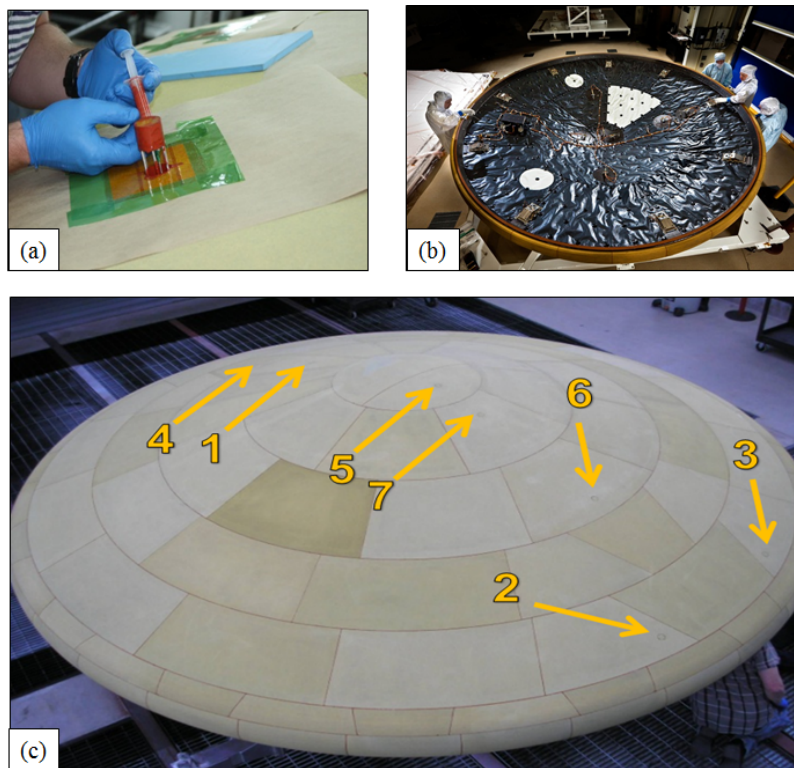


Figure 4 (a) Installation of a MISP plug with RTV-560 bonding agent, (b) MEDLI interface on the inner side of the heatshield, and (c) seven installed MISP plugs on MSL PICA heatshield.

MISP Science Objectives

To date much of the validation of Mars entry aerothermodynamic and TPS response has occurred via ground testing. The flight data obtained from MEDLI instrumentation suite will address many outstanding questions that cannot be addressed by ground testing in existing facilities. A set of science objectives listed below was formulated for the MISP instrumentation with the intent to reduce or improve some of the existing uncertainties.

1. Reconstruct Aeroheating: Construct the best estimate of the surface heating environment during hypersonic entry
2. Determine Leaside Turbulent Heating Levels and Augmentation: Using aeroheating reconstruction, determine turbulent heating levels and roughness augmentation in the leaside forebody of the vehicle to validate CFD predictions and correction factors
3. Determine Boundary Layer Transition Onset: Identify time of boundary layer transition to turbulence for validation of transition models and correlations
4. Determine Stagnation Point Heating Augmentation: Confirm or reject the presence of augmented heating at the stagnation point that is observed in several wind tunnel measurements
5. Measure Sub-Surface Material Temperature Response: Provide in-depth temperature measurements for material response model validation
6. Determine Total TPS Recession: Determine total recession of the PICA during hypersonic entry and validate recession model (confirm or reject fail margin)
7. Measure Depth of Isotherm in TPS: Using HEAT (isotherm) sensor data to provide isotherm temperature and isotherm depth versus time during hypersonic entry

MISP Sensor Error Budget and Arc Jet Testing

A set of qualification tests in arc jet facilities were conducted to ensure that integration of the sensor in the heatshield did not adversely impact the heatshield performance. Once qualified, subsequent ground testing was performed to characterize the sensor performance at nominal conditions and to quantify MISP measurement errors, biases, and uncertainties to aid in subsequent post-flight analysis of acquired data. An assessment of various instrumentation errors and sources of uncertainty was made based on numerous data sources from manufacturing, installation, laboratory tests, arc jet tests, simulations, and literature review. For MISP thermocouples, accuracy of EMF output, impact of thermal gradients, chemical interactions, thermal lag and perturbation, electrical shunting, bead location, etc., have been considered. For MISP HEAT sensors, uncertainties such as resistance measurement, sensed depth, thermal gradient correction, and inferred isotherm temperature have been considered.³

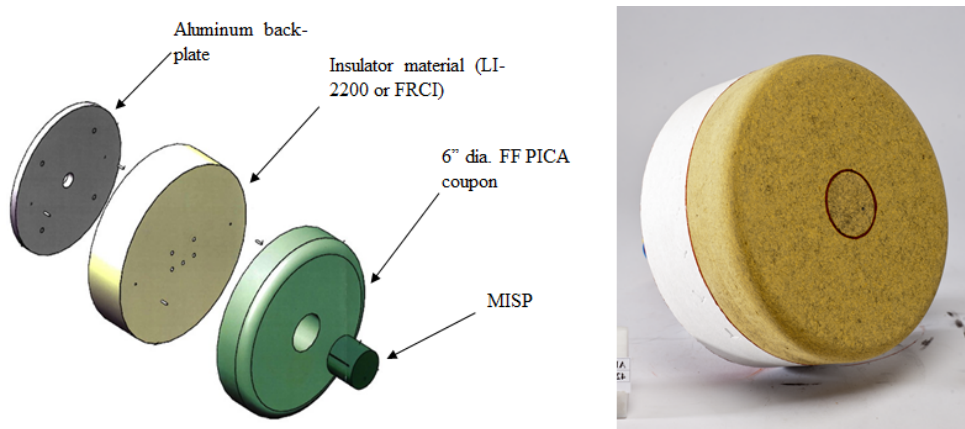


Figure 5 Arc jet test model for stagnation testing (a) material stack up and (b) a 6 in. flat-faced PICA model with a MISP plug bonded with RTV-560.

The arc jet testing was performed in stagnation as well as shear environments in the NASA Ames Arc Jet Test Complex. For stagnation testing the Aerodynamic Heating Facility (AHF) and Interaction Heating Facility (IHF) were used. All tests were conducted in air mixed with some Argon as the working gas. The capability to test in a CO₂ atmosphere was not available at this time, and it was not considered critical to meet the test objectives. The Ames Panel Test Facility

(PTF) was used for shear testing. Additional testing at Ames Turbulent Flow Duct (TFD) to achieve a turbulent flow environment has been planned. For arc jet testing MISP plugs, identical to the flight plugs, were installed in 15.2 cm (6 in.) diameter PICA coupons for stagnation testing (see Figure 5) and in 30.48 cm (12 in.) square PICA panels for shear testing. The test coupons, panels, and the MISP plugs were fabricated using the same billet of PICA that was used to manufacture the flight plugs to ensure consistency in material properties and reduce the variability that exists between billets.

MARS ENTRY ATMOSPHERIC DATA SYSTEM (MEADS) DEVELOPMENT

The MEADS concept is an implementation of a Flush Air Data System (FADS). The FADS concept was conceived and developed specifically to provide research quality air data during the hypersonic flight regime where the classical Pitot static probe could not survive. The pressure ports are arranged to provide a flush atmospheric data system from which aerodynamic data can be computed.

MEADS consists of seven 2.54 mm (0.1 in.) diameter pressure ports installed through the MSL PICA heat shield at strategic locations to acquire heatshield surface pressure data during the atmospheric entry phase at Mars. The MEADS pressure ports are located on the MSL heatshield as shown in Figure 1b. The predicted flow streamlines over the surface of the TPS are also shown in this figure. All of the pressure ports are located a minimum of 7.62 cm (3 in.) from the PICA tile seams to minimize the possibility of flow disturbances at the ports. At each of the pressure port locations there is a pressure transducer installed on the internal surface of the heatshield structure as illustrated in Figure 6.

Pressure ports P1 and P2 are located in the stagnation region to provide a nearly direct measurement of the total pressure in the high Mach regime. Ports P3, P4, and P5 lie on the spherical nose cap and are placed in order to take advantage of the simple geometry for angle-of-attack measurements. Additionally, P4, located at the geometric center, provides a nearly direct total pressure measurement at the low Mach regime prior to parachute deployment. The final two ports are located in the horizontal plane of symmetry, approximately 1.0 meter from the centerline. The ports P6 and P7 provide the off-axis measurements needed to estimate the angle of sideslip. The pressure ports are connected to pressure transducers via a stainless steel tube system illustrated in Figure 6. In addition a thermocouple is attached to the transducer shell to provide the transducer temperature.

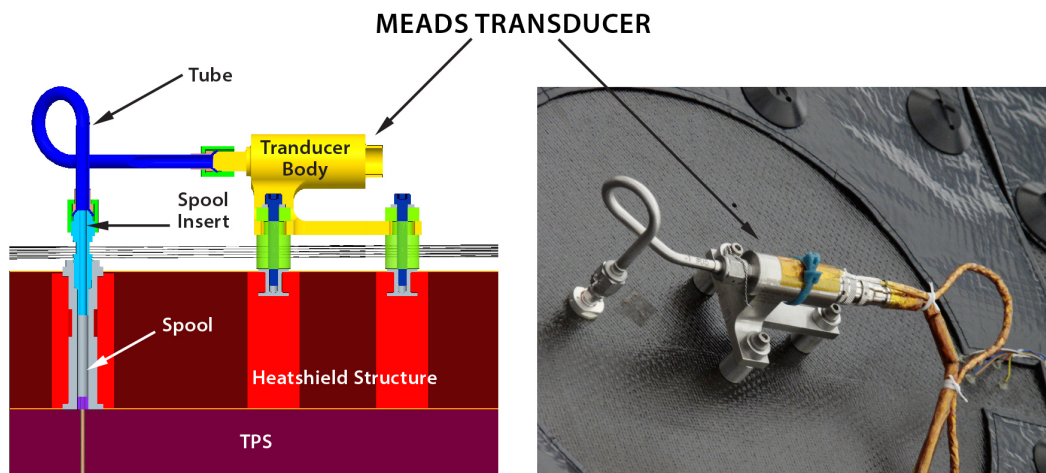


Figure 6 MEADS transducer and tube configuration

MEADS Science Objectives

A set of science objectives, listed below, was formulated for the MEADS instrumentation with the intent to reduce or improve some of the existing uncertainties. The basic MEADS science objectives are to reconstruct aerodynamic and atmospheric data from pressure measurements alone. When combined with the on-board Inertial Measurement Unit (IMU) data these measurements serve to enhance the MSL trajectory reconstruction and performance analysis, and enable a separation of the aerodynamics from the atmosphere, which prior to MEADS has not been achievable for a Mars Entry, Descent and Landing (EDL) reconstruction.

1. *Angle of Attack*: Estimate the angle of attack to within 0.5 degrees
2. *Angle of Sideslip*: Estimate the angles of sideslip to within 0.5 degrees
3. *Dynamic Pressure*: Measure dynamic pressure to within 2%, in a 3σ sense.
4. Secondary objectives are to estimate the Mach number, freestream density and atmospheric winds from the MEADS pressure measurements

MEADS Hardware and Arc Jet Testing

The MEADS pressure transducers are manufactured by Stellar Technologies, Inc. and are derivatives of off-the-shelf transducers. They are strain gage-type transducers with a range from 0 to 5 psia, outfitted at the manufacturer with flight electrical connectors, pressure input fittings, and mounting brackets. The transducers are not thermally compensated and they contain no electronics (electronics functions are performed by the SSE.) The transducers were calibrated with the SSE, as a subsystem, in combination with thermal/vacuum qualification at Langley. The calibration coefficients from this testing were then used to convert millivolts to pressures when the MEADS flight data was obtained. All of the hardware-related uncertainties were used in an error budget to ensure that the MEADS subsystem would meet the science objectives listed above.⁴ This process is described in detail in Reference 4.

In order for the MEDLI project to be allowed to install the MEADS pressure ports in the thermal protection heatshield, MSL required flight-like testing to demonstrate that pressure ports would not adversely affect the MSL spacecraft performance. Since pressure ports have never been installed in an ablating, planetary entry heatshield to measure surface pressures during entry, an extraordinary amount of arc jet testing was required to demonstrate compliance with MSL requirements. In addition, the MEDLI project needed to determine if pressures could be accurately measured in an ablating, pyrolyzing heatshield material. This resulted in a research and development test effort in addition to a demonstration test program to verify both the “do no harm” and the performance requirements of the pressure ports in the MSL heatshield.

SENSOR SUPPORT ELECTRONICS (SSE) DEVELOPMENT

The SSE conditions, digitizes, and then transmits information from the MSL heatshield sensors to the Descent Stage Power and Analog Module (DPAM). The SSE contains two active electronic boards housed in an aluminum chassis. The analog board contains the circuitry that converts thermocouple and pressure data analog data into digital signals. The digital board contains an ACTEL field programmable gate array (FPGA) that controls the analog-to-digital conversion and the RS-422 interface to the MSL DPAM. The digital board also provides conditioning of the 28V power provided by MSL and conversion to ± 15.0 V, 5.0 V and 2.5 V power needed by various electronics within the SSE.

The SSE samples thirty-one (31) thermocouples, six (6) recession sensors and seven (7) analog pressure transducer inputs. In addition, the SSE samples thirty-three (33) internal measurements devoted to health status and internal temperature monitoring. A multiplexer routes all in-

puts into a single, 14 bit analog-to-digital converter. Each data sample is 16 bits with two bits reserved for data synchronization. MEDLI generated approximately 0.9 MBytes during operations. The raw data rate from MEDLI to the DPAM is 4 kilobits per second. The DPAM added time tags (16 bits each) to each data frame resulting in an additional 225 Kbytes for 30 minutes of operation. The total MEDLI data volume was 1.1 MBytes. MEDLI was powered on approximately 5 hours before atmospheric interface, where data is transmitted over the MSL EDL-1553 bus for storage and real-time data processing (synchronizing, de-multiplexing, creating real-time data products, and running an aerothermal state monitor algorithm for triggering tones when given conditions are met) on the Rover Compute Element (RCE). The raw MEDLI data is stored in RCE memory until telemetered back to Earth after landing.

Each of the sensor subsystems are independently calibrated, and each contains its own two-point on-board fixed measurement that is used as a health check and to provide a self-calibration if required. The SSE signal conditioning is extremely linear and as a result, the conversion to engineering units from digital counts only requires a gain and offset term. For most measurements, the offset term is directly measured in flight, leaving the gain coefficients to be computed in post-flight analysis. For housekeeping data, this gain coefficient is fixed (static). However, for sensitive measurements such as pressure readings, the gain coefficient is computed as a multiple-order function with respect to the SSE temperature.

The SSE measures temperature from each thermocouple in the range of $-173\text{ }^{\circ}\text{C}$ – $1027\text{ }^{\circ}\text{C}$ to within $[\pm 2\text{ }^{\circ}\text{C}$ or 2% of thermocouple full-scale below $0\text{ }^{\circ}\text{C}$ and ± 1.1 degrees $^{\circ}\text{C}$ or 0.4% of thermocouple full-scale above $0\text{ }^{\circ}\text{C}$] for the entire operating range. Since the SSE reads voltage from thermocouples, the above requirement translates into an SSE accuracy of $\pm 521\text{ }\mu\text{V}$ below $0\text{ }^{\circ}\text{C}$ and $\pm 201\text{ }\mu\text{V}$ above. A worst-case temperature accuracy of $\pm 8.4\text{ }\mu\text{V}$ was measured, which is well below the required performance levels.

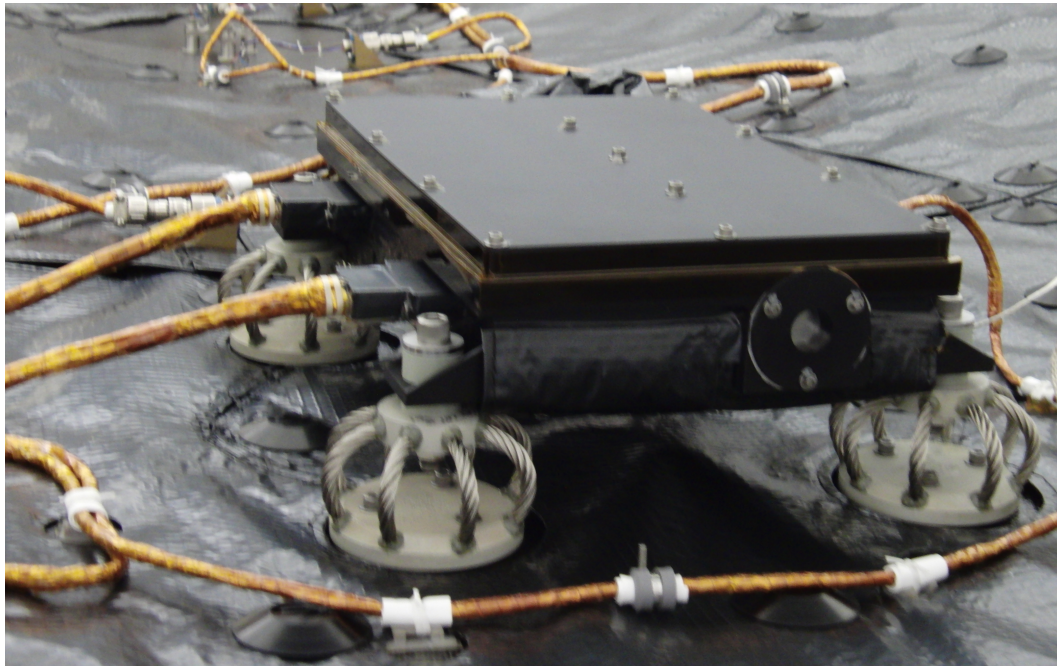


Figure 7 Sensor Support Electronics box and wire rope isolators integrated on MSL heatshield

MEDLI HEAT sensors measure the depth of a $700\text{ }^{\circ}\text{C}$ $[\pm 50\text{ }^{\circ}\text{C}]$ isotherm through the TPS material as a function of time, to within $\pm 0.50\text{ mm}$. HEAT sensors are based on resistance with a

typical conversion constant of 69 Ω /mm. To measure the resistance of the MISP HEAT sensors, a 1 mA constant current source is used to excite the sensor and the corresponding voltage is then measured. The accuracy requirement of ± 0.5 mm translates into a reading of ± 34.5 Ω by the SSE. Over the entire operating range, the measured accuracy was -2.5 to +1 Ω . To provide in-flight health and calibration information on the SSE circuitry, one channel monitors the reference voltage of the MISP circuits, and two on-board fixed precision resistors of 0 Ω and 1500 Ω are in-line and excited by the same 1mA current source as the HEAT sensors. The resulting voltage of these two fixed resistors constitutes the high and low check of the MISP HEAT system⁵.

Seven identical circuits condition the seven MEADS pressure transducer signals. The transducers use a Wheatstone bridge circuit to measure pressure that is excited by a 10V supply voltage. The SSE records the output of this bridge in millivolts. Each MEADS pressure input has its own individual signal conditioning electronics and is independently calibrated. To achieve the required measurement accuracy, the temperature of the SSE and the temperature of each MEADS transducer are recorded during flight, and used to determine these coefficients post-flight. Two internal SSE channels monitor the health of the MEADS temperature and pressure system. These on-board offsets are compared with the calibrated offsets based on the SSE temperature, and the health of the system is represented by small differences in these two numbers.

As an ancillary objective, the MEDLI data was used to determine whether or not the heatshield and flight vehicle remained in a nominally healthy state during entry descent and landing (e.g., expected temperatures, pressures, and heatshield recession rates close to those modeled in simulation). A select set of the 77 MEDLI channels were telemetered either direct-to-earth or via a Mars orbiter (depending on availability) in near real-time. In the event of a catastrophic failure of the heatshield during entry, this real-time data would have been extremely important to the reconstruction effort and failure investigation. In this investigation, the MISP thermocouples can be used to examine heatshield response including recession rate. The MISP HEAT sensors can be used for time dependent aerothermal and recession evaluation. The MEADS pressure ports can be used to examine dynamic pressure, atmospheric density, winds and vehicle orientation.

The real time data channels allocated to MEDLI (16 total) were equally divided between the two subsystems, MEADS and MISP. All 7 MEADS pressure sensors were sampled at 1Hz except MEADS Port #2 (near the stagnation point) was sampled at 2 Hz. MISP real time channels consist of 6 thermocouples (across 6 sensor locations on the heatshield) and 2 HEAT sensors (Plug #2 and Plug #3) were sampled at 1 Hz.

FLIGHT DATA ANALYSIS

MSL Entry Descent and Landing Overview

The MEDLI system was powered on approximately five hours prior to entry on August 5th, 2012 to allow the SSE to thermally stabilize before entry. MEDLI began to acquire data approximately ten minutes before entry with a subset of the critical MEDLI data transmitted real time during EDL and was operational until 10 seconds before heatshield separation. The real-time telemetry includes eight direct-to-Earth tones to indicate incremental progression of events. The full MEDLI dataset was stored in the Rover Compute Element (RCE) for transmission to Earth at a later time and was successfully received on Earth a few days after landing. Figure 8 shows a timeline of the six major EDL segments: Exo-Atmospheric, Entry, Parachute Descent, Powered Descent, Sky Crane, and Fly Away⁶. MEDLI was operational prior to cruise stage separation and through the parachute deployment.

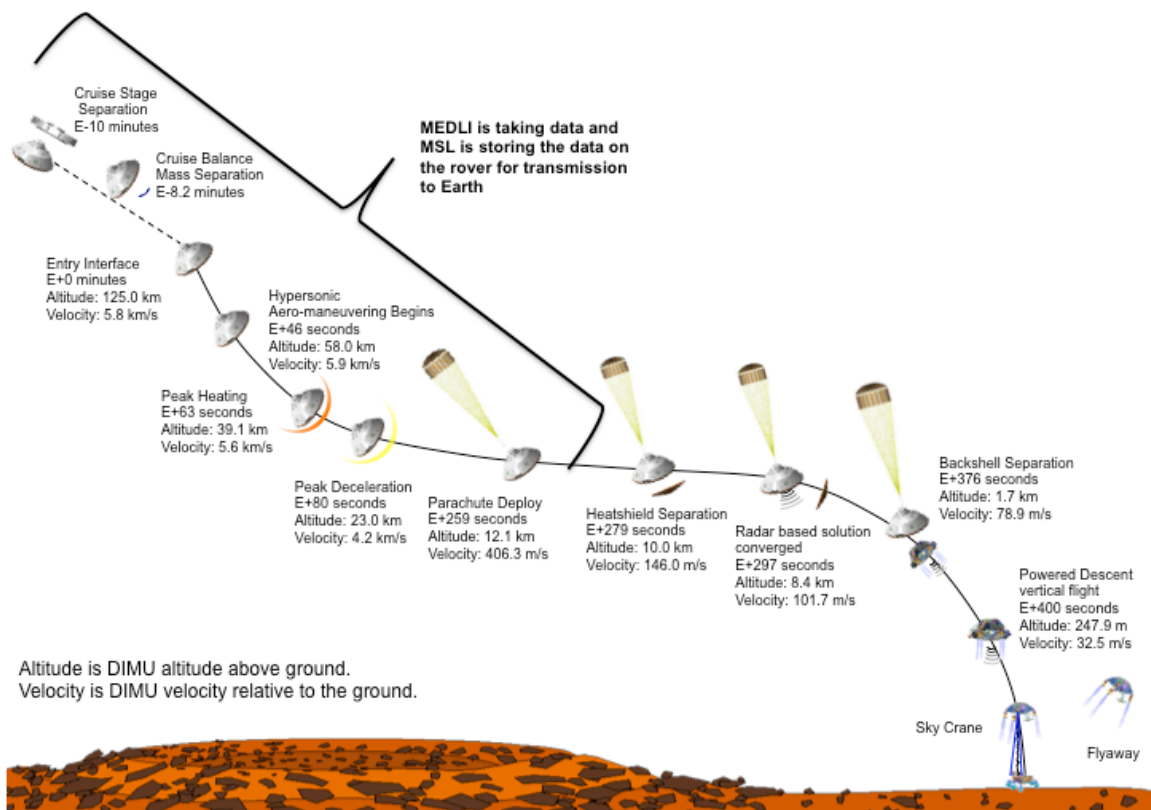


Figure 8 MSL entry, descent, and landing timeline

Initial MISP Observations

Figure 9 shows MISP thermocouple data acquired during MSL entry. All thermocouples performed according to expectations and returned virtually noise free data. It must be noted that MISP 5 and 7 only have two thermocouples wired due to an overall data volume constraint. A significant finding in the data is the survival of all near surface thermocouples throughout the heat pulse, suggesting a total TPS recession less than 2.54 mm (0.1 in.). The pre-flight model predictions showed the recession front moving beyond the depth of near surface thermocouples at MISP 2, 3, and 6.

Another readily noticeable feature in the thermocouple data is onset of turbulence, which can be identified by an abrupt change in the slope of the temperature traces. As flow over the heatshield transitions from laminar to turbulent, the heat flux jumps several fold, which is reflected in the data as an instantaneous change in the rate of temperature rise. The onset of turbulence before peak heating is apparent in all four leeside plugs (T2, T3, T6, & T7). The windside plugs do not show onset of turbulence, which is consistent with model predictions. The MEDLI data will enable validation of the augmented heating levels and the timing of transition from laminar to turbulent flow on the heatshield.

A direct comparison between nominal model predictions and thermocouple data is presented in Figure 10. In the stagnation region, at MISP 1 and 4, the peak temperatures at the near surface thermocouple is under predicted by about ~ 100 °C. The under prediction of the peak temperature could be due to a variety of reasons that are under investigation. The agreement of the model predictions with the deeper thermocouple temperatures is generally good. Similar to the stagnation plugs, the peak temperatures at MISP 5 and 7 are under predicted by models. At MISP 5 the peak

predicted temperature is lower by about ~ 100 °C for the top thermocouple, whereas at MISP 7 the under prediction is exacerbated by an early boundary layer transition. The peak temperature at MISP 7 is ~ 210 °C greater than model predictions.

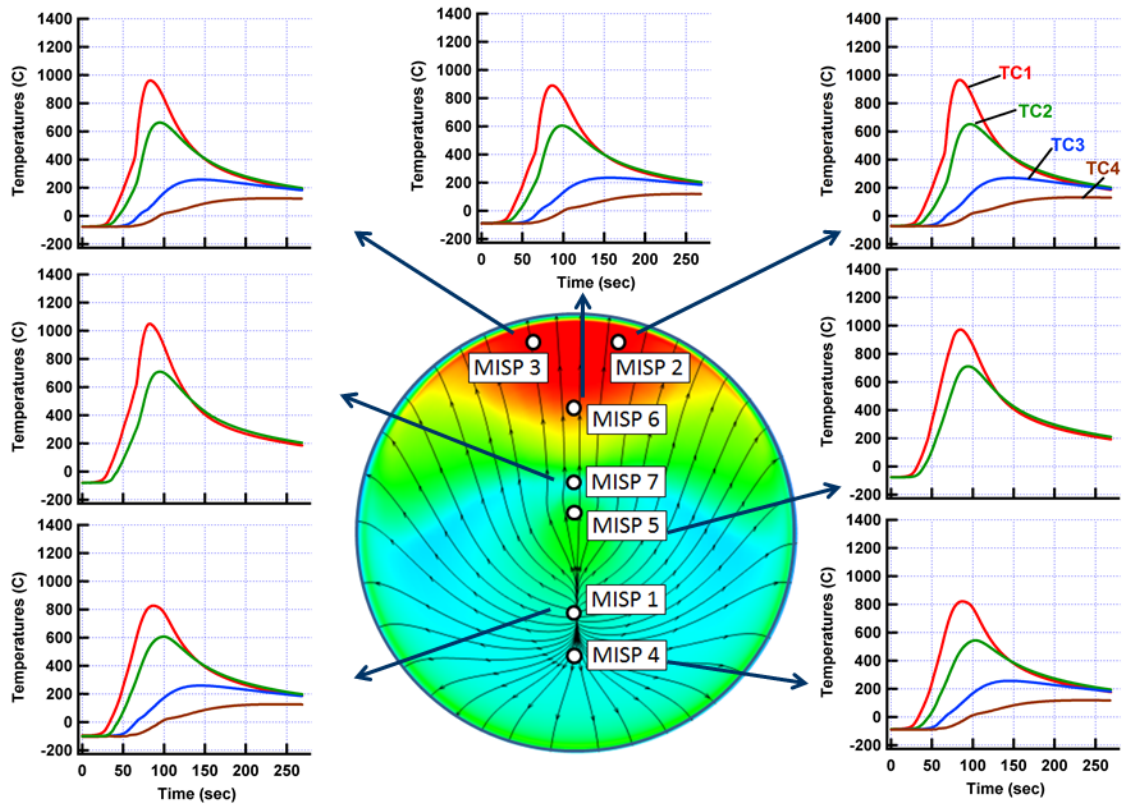


Figure 9 MISP thermocouple data obtained during MSL entry. TC1, TC2, TC3, and TC4 represent thermocouples at nominal depths shown in Figure 2a.

The leeside of the vehicle forebody clearly experienced turbulent heating. Initial comparisons of the temperature data shows that, unlike other regions of the heatshield, the predicted peak temperatures are much higher than measurement. In fact, the top thermocouple temperature in model prediction rises until the surface recession front reaches the thermocouple depth, which is nominally 2.54 mm (0.01 in.). In flight, however, the recession front does not reach the top thermocouple. Recession and the proximity of the top thermocouple to the ablator surface are critical factors that need to be assessed before reasonable predictions of the top thermocouple temperatures are made. The other reasons for higher predicted temperatures are early onset of turbulence in the leeside region and a possible deficiency of the turbulence model used. All of the above factors are under investigation.⁷

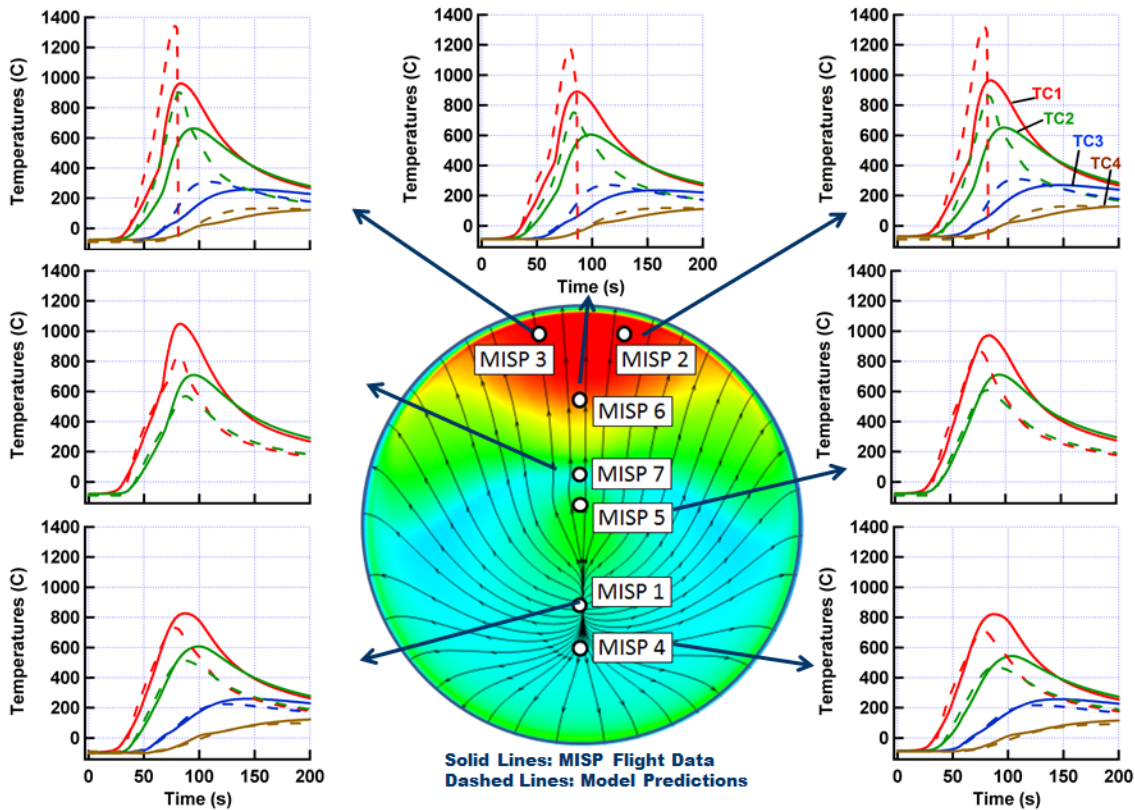


Figure 10 MISIP thermocouple data obtained during MSL entry compared with nominal (unmargined) model predictions.

Initial MEADS Observations

The raw MEADS pressures acquired during MSL EDL are shown in Figure 11. These pressures are based on the MEADS transducer outputs and pre-flight thermal vacuum chamber calibrations. An in-flight zero, or vacuum reference value was obtained prior to the MSL atmospheric entry, was applied to remove transducer bias. In general the pressure data are clean with little noise, until the time of the entry ballast mass ejections prior to parachute deployment. These shock events introduced vibrational noise into the pressure data. These noise spikes were edited out and filled in using linear interpolation, and a 1 Hz optimal Fourier filter was applied to smooth the data. The measurements were then interpolated to the Port 4 measurement times in order to produce pressures with common time tags.

The MEADS measurements were processed using a nonlinear least-squares algorithm to produce estimates of angle of attack, angle of sideslip, dynamic pressure, and static pressure. The least-squares algorithm includes a novel IMU-aiding approach in which the IMU velocity is used to improve the estimate of Mach number. Atmospheric density is computed from the dynamic pressure estimate and the IMU velocity, assuming no winds. The MEADS dynamic pressure and IMU acceleration and angular rate measurements can also be combined to produce estimates of the vehicle aerodynamic forces and moments⁸. Further details on the MEADS processing algorithms can be found in Reference 8.

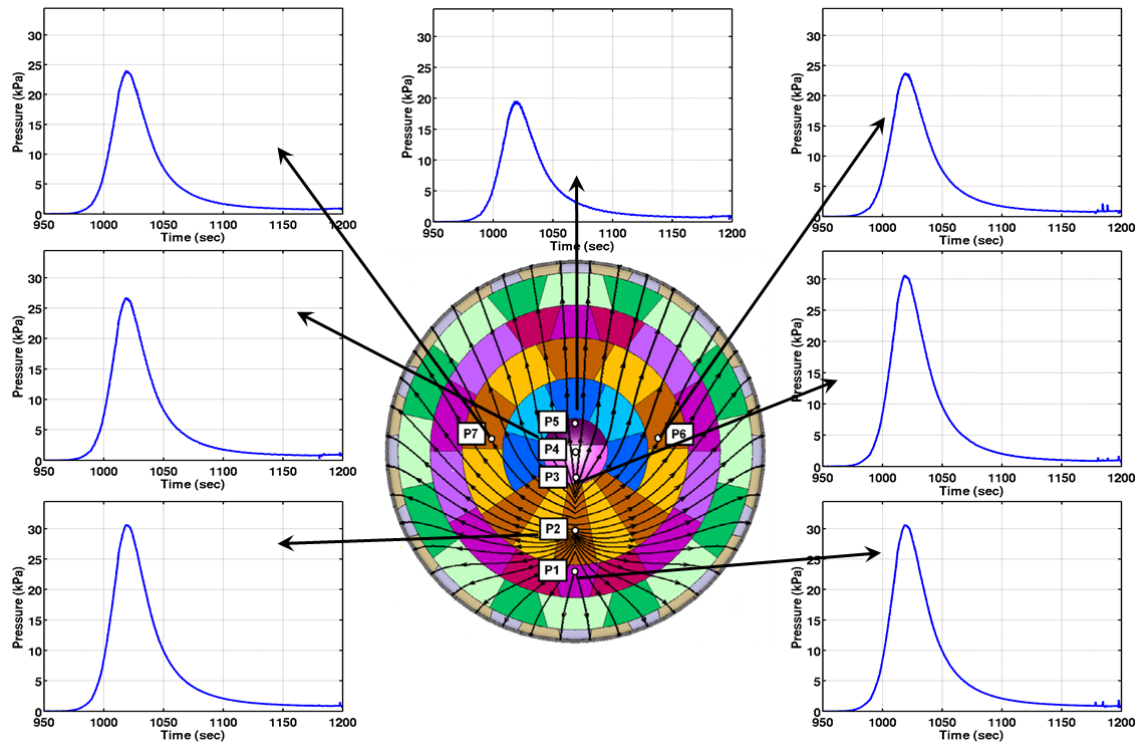


Figure 11 MEADS measurement data during EDL

Results of the MEADS reconstruction are shown in Figure 12-Figure 14. Figure 12 shows results for the angle of attack estimate, compared to the on board navigation estimate and results from a reconstruction using the vehicle nominal aerodatabase and ratios of accelerations. There are differences between the reconstructions on the order of 0.4 degrees in the hypersonic regime, with better agreement in the supersonic regime. A suspected wind event occurs at a time of approximately 680 seconds (at an altitude of 13-14 km) where the inertial angle of attack differs somewhat from the atmospheric relative angle of attack. There is additional evidence of this wind disturbance from the response of the vehicle to guidance commands.

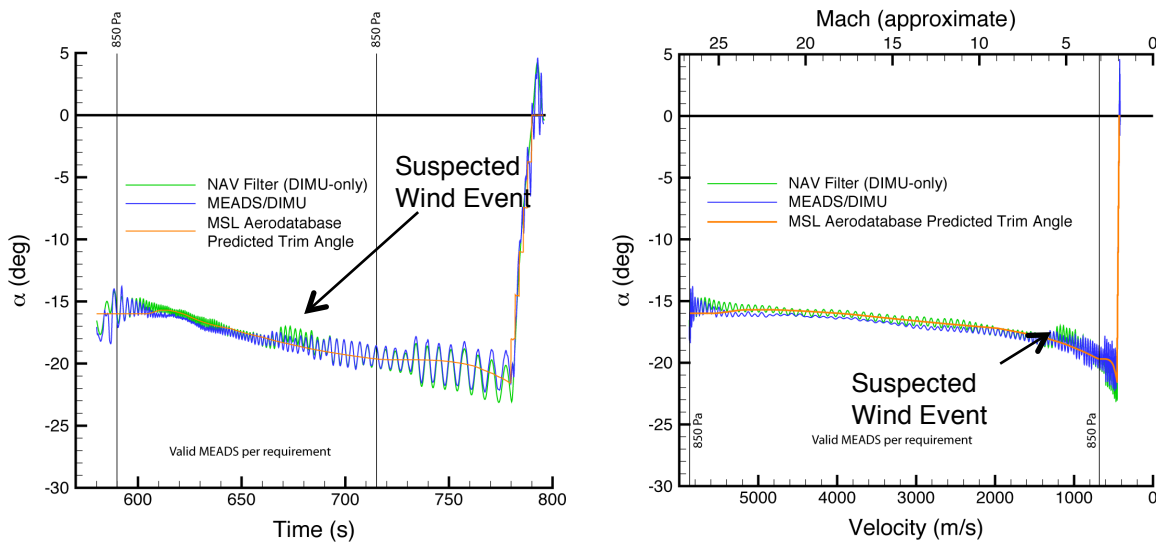


Figure 12 MSL angle of attack reconstructed with MEDLI data

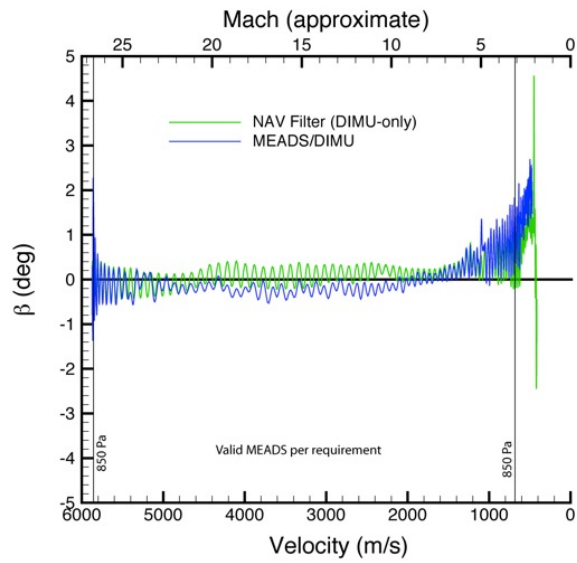


Figure 13 MSL angle of sideslip reconstructed with MEDLI data

The sideslip angle estimates are shown in Figure 13. The MEADS reconstruction is in good agreement with the navigation solution. The reconstruction indicates that the sideslip angle remained small over the trajectory, as expected. Both reconstructions show a slight positive trend in the supersonic regime.

Figure 14 shows results for the axial force coefficient. Here, the MEADS reconstruction is compared with the nominal aerodatabase queried along the MEADS-derived trajectory, along with the $\pm 3\sigma$ bounds. There is an approximate 2% difference between the MEADS reconstruction and the nominal aerodatabase over most of the trajectory. This difference can be reconciled with reasonable dispersions of 0.4σ in the hypersonic regime and 0.25σ in the supersonic regime. Additionally, a small correction to the base drag parameter can further reconcile differences in the low supersonic regime.

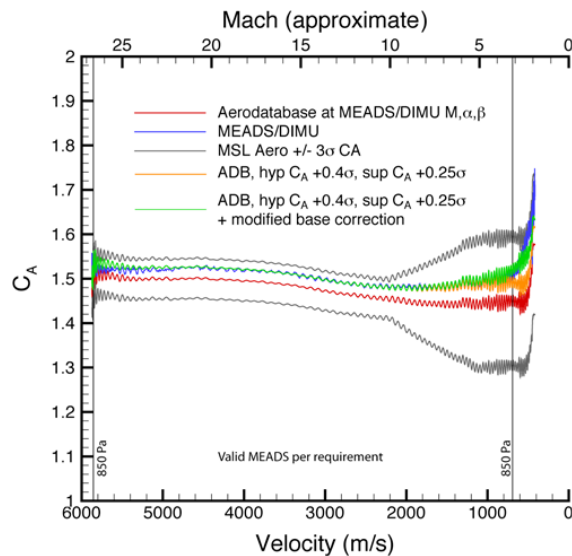


Figure 14 MEADS measured axial force coefficient (C_A)

CONCLUSION

The MEDLI system gathered the first comprehensive set of heatshield temperature and pressure readings on an entry vehicle at Mars during the MSL entry and descent. The MEADS subsystem successfully acquired a set of high quality pressure data during MSL's entry and descent, collecting data from before atmospheric interface through parachute deploy. A pressure-based reconstruction is enabled by the pressure measurements from seven pressure ports on MSL's heatshield. Such heatshield pressure data has not successfully been collected during Mars entry prior to Mars Science Laboratory. An important feature of the new pressure-based reconstruction technique is that it enables an atmosphere reconstruction to be conducted without assumptions on the vehicle aerodynamics. This in turn allows for an aerodynamic reconstruction to be performed that has not been possible for previous Mars entry trajectory reconstructions.

The MISP subsystem successfully acquired heatshield temperature data and all the thermocouples returned reasonable data with virtually no noise. The initial assessment of MISP temperature data has provided valuable insights and highlighted areas for further analysis and investigation. Future work is directed toward meeting the science objectives that require assessments of boundary layer transition, stagnation point heating, turbulent heating augmentation, surface recession, and in-depth thermal response. Current thermal protection system design margins that are based solely on ground test data will be re-assessed using MEDLI data. It is anticipated that margins applied for surface recession, turbulent heating, stagnation point heating will be significantly improved and strongly substantiated.

REFERENCES

- ¹ Gazarik, M. J., Wright, M. J., Little, A., Cheatwood, F. M., Herath, J. A., Munk, M. M., Novak, F. J., and Martinez, E. R., "Overview of the MEDLI Project," IEEE 2008 Aerospace Conference, March 2008.
- ² Gorbunov S. et al. "Thermal Protection System Ablation Sensor," US Patent 8,069,001 B1, November 29, 2011.
- ³ Santos, J., White, T., and Cozmuta, I., "MSL Entry, Descent, and Landing Instrumentation-MISP Error Budget Report," Document No. MEDLI-0236, February 2011.

⁴ Karlgaard, C. D., Beck, R. E., O’Keefe, S. A., Siemers, P. M., White, B. A., Engelund, W. C., and Munk, M. M., “Mars Entry Atmospheric Data System Modeling and Algorithm Development,” AIAA Paper 2009-3916, June 2009.

⁵ Antill, C., “SSE-007 Performance Report,” Document No. MEDLI-0230, October 2010.

⁶ Steltzner, A. D., Burkhart, P. D., Chen, A., Comeaux, K. A., Guernsey, C. S., Kipp, D. M., Lorenzoni, L. V., Mendeck, G. F., Powell, R. W., Rivellini, T. P., San Martin, A. M., Sell, S. W., Prakash, R., and Way, D. D., “Mars Science Laboratory Entry, Descent, and Landing System Overview,” 7th International Planetary Probe Workshop, Barcelona, Spain, June 2010.

⁷ Bose, D., White, T.R., Santos, J.A., Feldman, J., Mahzari, M., Olson, M., Laub, B. “Initial Assessment of Mars Science Laboratory Heatshield Instrumentation and Flight Data,” 51st AIAA Aerospace Sciences Meeting, January 2013.

⁸ Karlgaard, C., Kutty, P., Schoenenberger, M., Shidner, J., and Munk, M., “Mars Entry Atmospheric Data System Trajectory Reconstruction Algorithms and Flight Results,” AIAA Paper 2013-0028, 51st AIAA Aerospace Sciences Meeting, January 2013.